ACS APPLIED MATERIALS & INTERFACES

www.acsami.org

Research Article

Low-Temperature Barrier Discharge Plasma Modification of Scaffolds Based on Polylactic Acid

Olesya A. Laput, Irina V. Vasenina, Yelena G. Shapovalova, Andrey N. Ochered'ko, Aleksandr V. Chernyavskii, Sergey V. Kudryashov, and Irina A. Kurzina*

Cite This: https://doi.org/10.1021/acsami.2c11027

Read Online

ACCESS | Metrics & More | Article Recommendations

ABSTRACT: We have explored the effect of low-temperature barrier discharge plasma treatment in oxygen, nitrogen, and argon on modification of the physicochemical properties of polylactic acid (PLA)-based scaffolds. The cellular-mediated immune response to the interaction of macrophages of three donors with the modified surface of PLA-based scaffolds was also investigated. Carbonization of the PLA surface accompanied by a carbon atomic concentration increase is shown to occur following plasma treatment. Argon plasma significantly affects the wettability characteristics of PLA; the hydrophilicity and lipophilicity are improved, and the surface energy is increased. The viability of cells in the presence of plasma-modified PLA scaffolds is lower than that for unmodified PLA but remains greater than that for the negative control. We find that PLA scaffolds do not cause increased expression of the proinflammatory (TNFα, IL-6, IL-1β) cytokines after 6 days of cell cultivation. At the same time, PLA scaffolds do not affect the increased production of anti-inflammatory cytokines (IL-10).

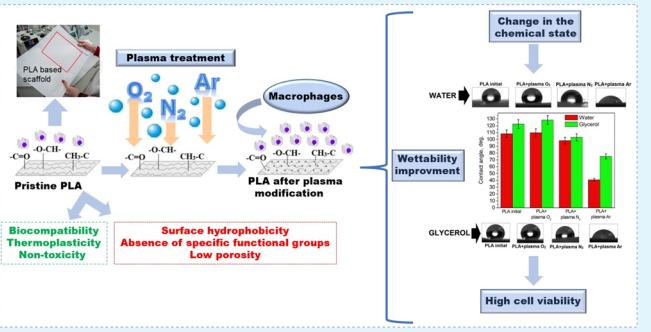

KEYWORDS: *polylactic acid, low-temperature plasma, barrier discharge, chemical compound, wettability, free surface energy, cell viability, macrophage activation, cytotoxicity*

1. INTRODUCTION

The interaction of implants with organisms is an important issue in regenerative medicine because there is always a risk of an inflammatory response that interferes with recovery. Despite progress in biomedical materials science, resorbable implants for soft tissue reconstruction with predictable physicochemical and immunomodulatory properties are not currently available in clinical practice.[1] Most implants for soft tissue reconstruction or precise drug delivery utilize polymer-based scaffolds, specifically from polylactic acid (PLA).[2] PLA is an aliphatic polyester frequently used in biomedicine for its biocompatibility and nontoxicity of both PLA and its degradation products.[3,4] However, the main disadvantages of PLA are its lack of porosity and the "inertness" of the surface—its hydrophobicity and absence of specific functional groups for cell attachment and growth. This drawback can be resolved by production of PLA-based materials by electrospinning[5] and low-temperature plasma treatment[6] of these scaffolds.

Important advantages of plasma-modified scaffolds over classic implantology materials include the reduced risk of undesirable immune reactions in the tissue surrounding the implant and the presence of the necessary set of surface functional groups and physicochemical properties, in which the material is acquired in the process of plasma treatment.[7] Low-temperature plasma treatment and plasma deposition techniques are advantageous surface modification technologies by virtue of their environmental friendliness, economy, and effectiveness for further medical application, because they can change the surface chemical state without altering the bulk properties. Oxygen, argon, and nitrogen plasma treatment is an established approach for modifying the chemical and elemental compositions of the PLA scaffold surface.[8] It has been shown that plasma treatment of PLA surfaces leads to an increase in oxygen-containing (carboxyl) functional groups that influence surface wettability and contribute to cell adhesion and viability on the PLA-modified surface.[9]

The aim of the work described here was to investigate the effect of oxygen, argon, and nitrogen low-temperature plasma treatment on the physicochemical properties and biocompatibility of PLA-based scaffolds.

Received: June 21, 2022
Accepted: August 26, 2022

2. MATERIALS AND METHODS

2.1. Production of PLA-Based Scaffolds. PLA for electrospinning and further plasma treatment was obtained from *l*-lactide initial monomer synthesized in the Laboratory of Polymers and Composite Materials at Tomsk State University using the technique described elsewhere.[10] The average molecular weight of the PLA obtained was 150,000 g/mol. Scaffold formation was performed using Nanon-01 (MECC CO, Japan) electrospinning equipment with a cylindrical collector 200 mm in diameter at an average temperature of 23 °C in the chamber and relative humidity φ = 15%. A simplified schematic of the experimental setup is shown in Figure 1.

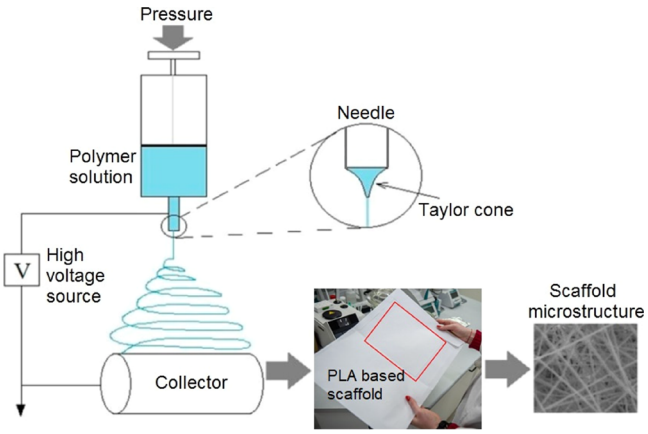

Figure 1. Schematic of the polymer electrospinning process.

The primary process parameters were: forming voltage—20 kV, solution feed rate—3 mL/h, solution volume—10 mL, scaffold width—50 mm, collector rotation—50 rpm, distance between needle and collector—130 mm, and needle diameter—1.3 mm (18 G), with no needle cleaning. The canvas was cut with a scalpel along the collector rotation axis, and the material was removed from the collector. Prior to plasma treatment, the scaffolds were placed in a vacuum chamber at a pressure of 10^{-2} Pa for 10 h at T = 100 °C to remove residual solvents.

2.2. Plasma Treatment of PLA-Based Scaffolds. PLA-based scaffolds obtained by electrospinning were treated with low-temperature barrier discharge plasma using a plasma-chemical reactor of planar geometry. A simplified schematic of the experimental setup is shown in Figure 2.

Plasma-forming gas (oxygen, nitrogen, or argon) from gas tank (1) is fed into the discharge chamber (3) through flow controller (2). The PLA sample is positioned between the HV (4) and ground (6) electrodes. The HV electrode (copper foil) is covered with a dielectric layer, a 2 mm thick glass fiber laminate (5); the ground electrode is cut from a solid bar of brass and serves as the massive horizontal base of the reactor. The PLA sample is located on the surface of the ground electrode facing the HV electrode inside the discharge chamber of the plasma-chemical reactor. The AC power source (7) initiates a discharge in the gap between the electrodes. The PLA plasma treatment conditions are shown in Table 1. The discharge power for different plasma gases differs, which leads to some variability in the surface physicochemical properties of the PLA-based scaffolds.

The voltage pulse formed by the AC power source is monitored using a Tektronix TDS 380 2-channel digital oscilloscope (Figure 2, 8) via a resistive HV probe (1810:1 division ratio) (Figure 2, 9) and a capacitive probe (Figure 2, 10). The discharge current I_D was determined from the first derivative of the capacitive voltage waveform $V_C(t)$. The transferred charge Q between the electrodes was evaluated as the product of the capacitive voltage V_C and the capacitance C_P (309 nF). Time dependencies of the transferred charge $Q(t)$ and the corresponding capacitive voltage $V_C(t)$ were used to construct Lissajous figures, the area of which is the discharge energy per pulse. The discharge power P_D is calculated from the product of the transferred charge Q per pulse and the pulse voltage V_{HV} multiplied by the pulse repetition rate f_{Hz}. The discharge powers for different plasma-forming gases are given in Table 1. The waveforms for a typical HV pulse, a discharge current pulse, and a capacitive voltage probe signal, and the barrier discharge Lissajous figure are shown in Figure 3.

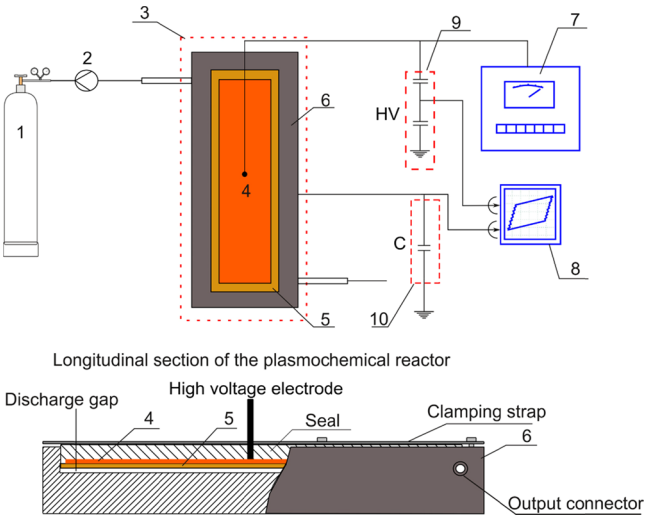

Figure 2. Schematic of the experimental setup for low-temperature barrier discharge plasma treatment of PLA-based scaffolds. 1—gas cylinder; 2—flow controller; 3—plasma-chemical reactor; 4—high-voltage (HV) electrode; 5—dielectric barrier; 6—ground electrode; 7—AC power source; 8—oscilloscope; 9—HV probe (1810:1); and 10—capacitive probe (309 nF).

Table 1. PLA Plasma Treatment Conditions

plasma-forming gas	O_2	N_2	Ar
plasma gas consumption, cm^3/s	60		
exposure time, t, s	120		
high-voltage electrode area, cm^2	10		
pulse duration, T, μs	500		
pulse repetition frequency, f_{Hz}, kHz	2		
high-voltage pulse height, V_{HV}, kV	7		
discharge power P_D, W	7.0	8.8	6.0

2.3. Investigation Techniques. *2.3.1. Chemical Composition.* The surface elemental composition was examined by X-ray photoemission spectroscopy (XPS) using a PHIX-tool automated XPS microprobe with a KαAl source. A monochromatic X-ray source was used, with a 400 μm^2 X-ray spot. A standard charge compensation system with low electron and ion energy (~0.1 eV) was used for analysis. Casa XPS (Casa Software Ltd.) software was used for data analysis.

2.3.2. Wettability. Ethylene glycol and glycerol contact angles were measured by a sessile drop technique using a Kruss Easy Drop (DSA25) instrument. Surface energy calculation was performed using the Owens−Wendt equation.[11]

2.3.3. Morphology. Microphotographs of the PLA surface in its initial state and after plasma treatment were obtained using a Carl Zeiss Axio imager Vario optical microscope in transmitted light mode.

The main clinical problem with the use of implantable materials is inflammation, both acute and chronic. The cells that can both stimulate and suppress inflammatory reactions in the implant microenvironment are tissue macrophages. Macrophages provide an immediate response to the penetration of a foreign pathogenic agent into the body, are key cells of the innate immunity system, and participate in the launch and implementation of reactions of the acquired immunity system.[12]

https://doi.org/10.1021/acsami.2c11027
ACS Appl. Mater. Interfaces XXXX, XXX, XXX−XXX

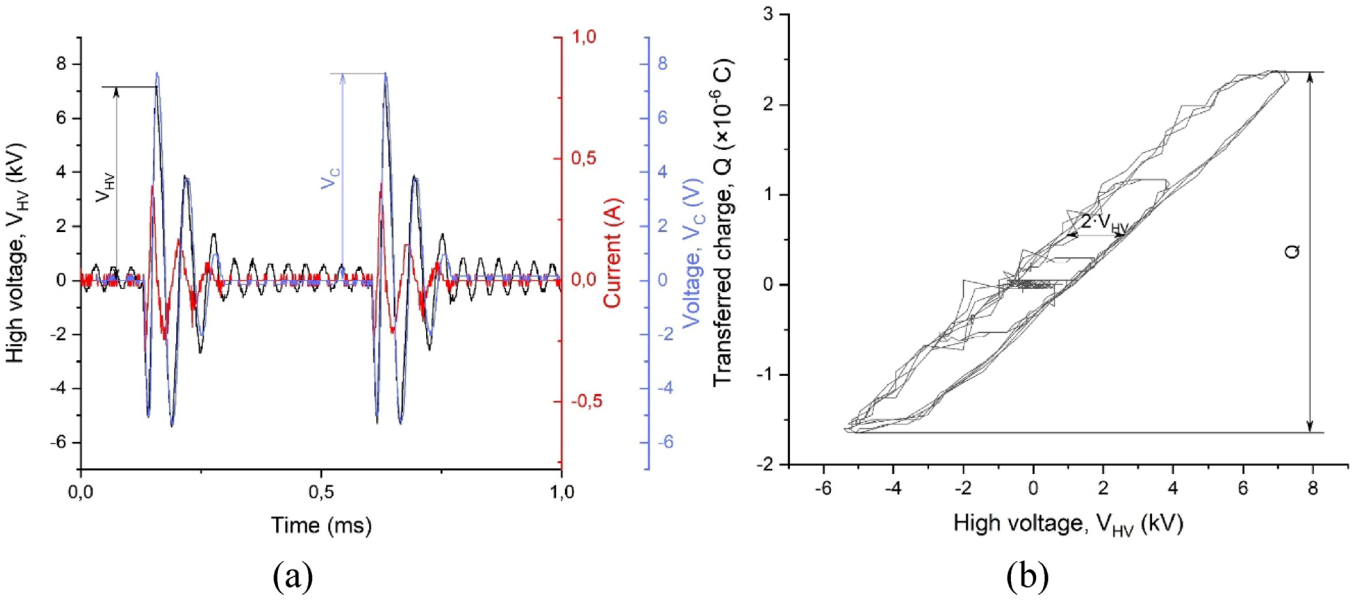

Figure 3. (a) Typical HV, discharge current, and capacitive voltage probe waveforms; (b) barrier discharge Lissajous figures for different gases (argon, oxygen, nitrogen).

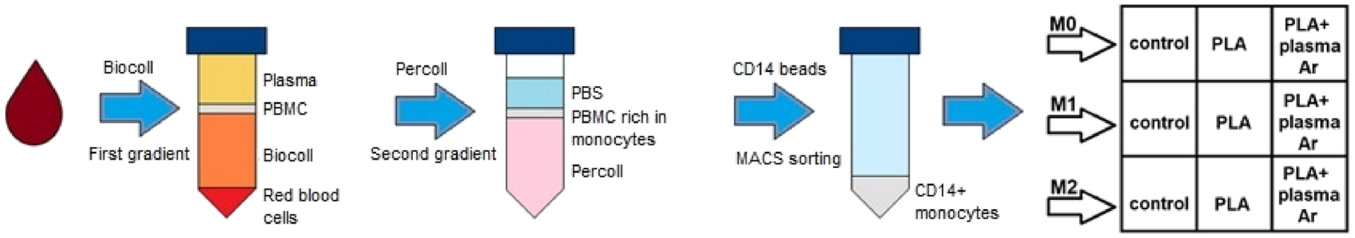

Figure 4. Isolation and activation of monocytes from buffy coat for the study of biocompatibility of polymeric materials.

2.3.4. Monocyte Isolation and Culture. Monocytes were isolated from the buffy coats of healthy donors[13] obtained from the Blood Transfusion Department of the Northern Clinical Hospital (Seversk, Russia). These monocytes were cultured at a concentration of 10^6 cells/mL in X-VIVO 10 medium (Lonza, Belgium) supplemented with 1 ng/mL M-CSF (Peprotech, Germany) and 10^{-8} M dexamethasone (Sigma-Aldrich, Germany). Scaffolds were cut into 0.7 cm^2 square-shaped pieces and UV-sterilized. The materials were placed in the wells of a 12-well plate; cells cultured without material were used as a control. Two milliliters of cell suspension containing 2 × 10^6 monocytes were added to each well. Isolated monocytes were immediately stimulated with cytokines: IFNγ—100 ng/mL (Peprotech, Germany) for M1 activation of monocytes and IL-4—10 ng/mL (Peprotech, Germany) for M2 activation and cultured for 6 days in a CO_2 incubator at 37 °C (Figure 4). Primary nonactivated macrophages were marked as M0.

2.3.5. Enzyme-Linked Immunosorbent Assay (ELISA). 1.5 mL of supernatants was collected after 6 days of cell culture. The concentration of human IL6, IL1β, IL10, and TNFα (VECTOR BEST, Russia) in the cell culture supernatants was measured by ELISA according to the manufacturer's instructions.[14] All samples were analyzed in duplicate. Data for three individual donors were presented for cytokine concentration measured on day 6. Measurements were performed with a Tecan Infinite F50 microplate reader (Tecan, Switzerland) at 620 nm wavelength.

2.3.6. Alamar Blue Assay. The viability of cells was assessed after cultivation (evaluation of metabolic). Alamar Blue fluorescent assay (Sigma, USA) was used to evaluate cell viability of nonstimulated monocytes cultured on day 6. To perform the analysis, 0.5 mL of cell culture medium was left in each well, and Alamar Blue was added (volume of Alamar Blue/medium equal to 1/10). Cells cultured without the material were used as a positive control. As a negative control (no living cells), X-VIVO serum-free medium with the addition of Alamar Blue was used. Cells were incubated with Alamar Blue for 24 h at 37 °C in a CO_2 incubator. The supernatants were then collected in a 96-well plate, and fluorescence intensity was analyzed using a Tecan Infinite 200 microplate reader (Tecan, Switzerland) (excitation 570 nm, emission 600 nm). All measurements were performed in triplicate.

3. EXPERIMENTAL RESULTS

3.1. Chemical Composition of the Surface. Figure 5 shows C1s spectra of PLA in its initial state (Figure 5a), and after oxygen (Figure 5b), nitrogen (Figure 5c), and argon (Figure 5d) plasma treatment.

The results (Figure 5 and Table 2) show that plasma treatment with all plasma-forming gases leads to a reduction of the content of oxygen-containing bonds in the PLA C1s spectra. This is indicative of polymer chain destruction processes. The Table 2 data show that the content of carbon bonds in coordination 1 ($-CH_3-C$) increases, but the content of carbon bonds in coordination 3($-O-C=O$) decreases by a factor of up to 1.3 after oxygen, nitrogen, and argon plasma treatment, while the content of carbon bonds in coordination 2($-O-CH-$) does not change significantly. Note that no new bonds in the PLA surface layer are formed by the plasma treatment.

XPS spectra of the PLA surface before and after plasma modification are shown in Figure 6. These spectra reveal the presence of the main PLA elements—carbon and oxygen, but a new peak with binding energy ~399.9 eV, corresponding to atomic nitrogen, appears following nitrogen plasma treatment. The atomic nitrogen content is 1.60 at %. We find that the carbon atomic concentration increases after plasma modification because of the reduction of oxygen atomic

https://doi.org/10.1021/acsami.2c11027
ACS Appl. Mater. Interfaces XXXX, XXX, XXX−XXX

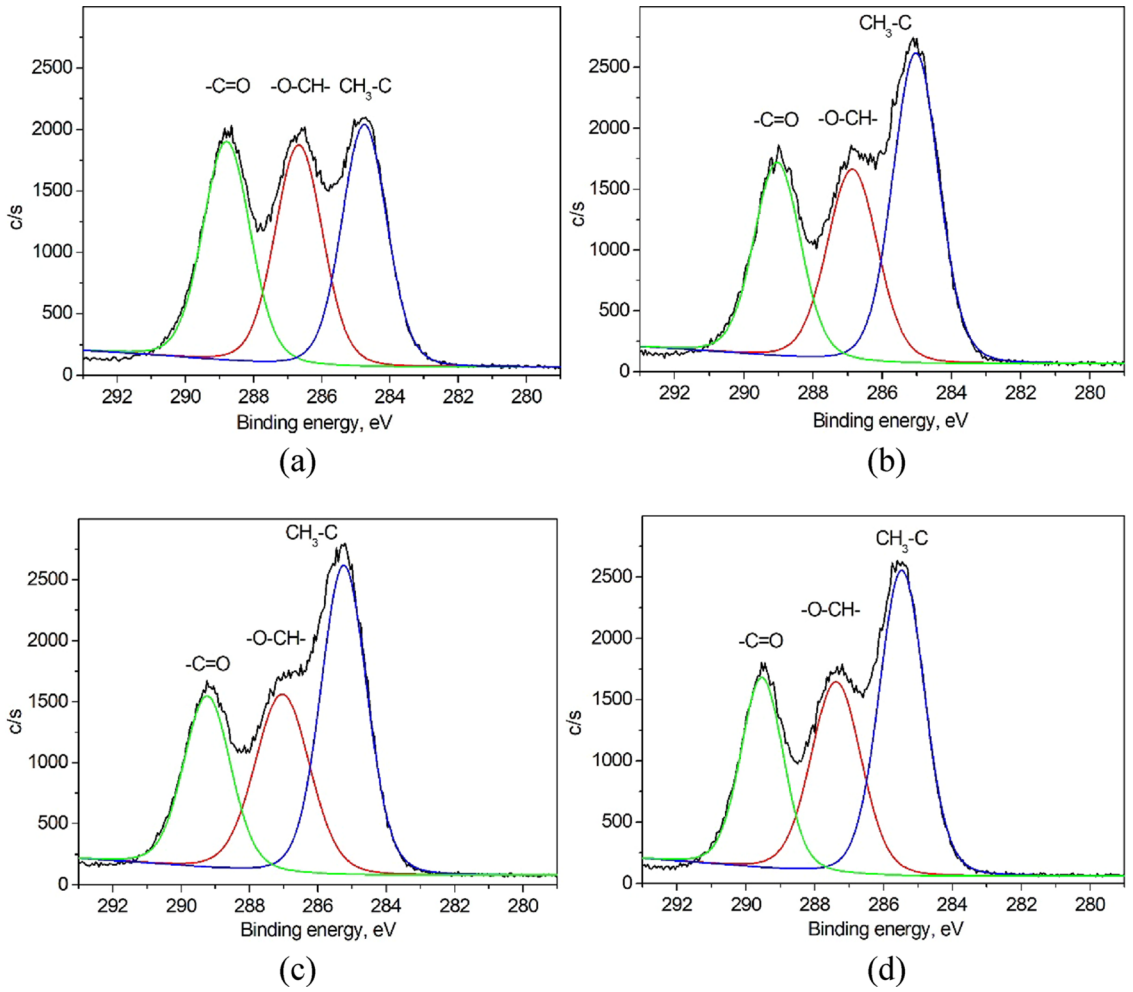

Figure 5. XPS spectra of initial PLA (a) and after plasma treatment in the flows of oxygen (b), nitrogen (c), and argon (d).

Table 2. Position of C1s Lines and Content of Bonds in PLA

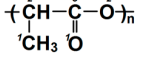	content of bonds in C1s spectrum, at %		
	1 (CH_3–C)	2 (–O–CH–)	3 (–O–C═O)
sample / binding energy, eV	285.00	286.98	289.06
PLA initial	34.54 ± 1.72	32.85 ± 1.64	32.61 ± 1.63
PLA + plasma O_2	43.38 ± 2.16	29.29 ± 1.46	27.33 ± 1.36
PLA + plasma N_2	44.25 ± 2.21	30.53 ± 1.52	25.22 ± 1.26
PLA + plasma Ar	43.92 ± 2.19	30.48 ± 1.52	25.59 ± 1.27

concentration (Table 3). The atomic ratio [C, at %]/[O, at %] increases for oxygen and argon plasma treatment, indicating surface carbonization.

3.2. Wettability of PLA. The results of contact angle measurements are shown in Figure 7. The initial (unmodified) PLA water contact angle is 110°, indicating that the surface is hydrophobic. Oxygen plasma modification of the PLA surface results in an increased contact angle (~2%), while nitrogen plasma treatment leads to a slight decrease (~9%). The PLA water contact angle is reduced significantly (~62%) by argon plasma modification, rendering the PLA surface hydrophilic, (41° the contact angle is less than 90°). Figure 7 also shows the PLA glycerol contact angle following plasma treatment. The initial PLA surface is oleophobic because the glycerol contact angle, 122°, is greater than 90°. The contact angle is increased slightly by oxygen plasma treatment and decreased by nitrogen plasma exposure. The glycerol contact angle is 76° for argon plasma-treated PLA, and the material is thus oleophilic.

Surface energy calculations reveal an enhancement of total surface energy from 6.44 mN/m to 26.68, 57.38, and 201.44 mN/m following oxygen, nitrogen, and argon plasma treatment, respectively. Both the polar and dispersive components of surface energy increase, with the polar component increase greater than the dispersive component (Figure 8). This effect is confirmed by XPS data that show an increase of oxygen-containing (carbonyl) groups and is probably associated

https://doi.org/10.1021/acsami.2c11027
ACS Appl. Mater. Interfaces XXXX, XXX, XXX−XXX

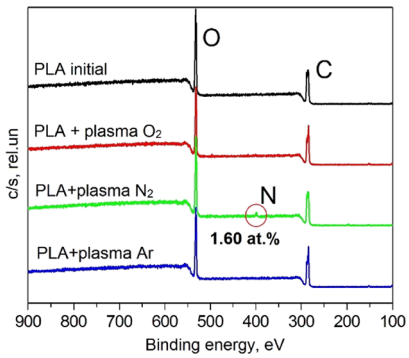

Figure 6. XPS spectra of PLA before and after plasma exposure.

Table 3. Atomic Ratio [C, at %]/[O, at %] of PLA before and after Plasma Modification

sample	ratio of atomic concentrations [C, at %]/[O, at %]	atomic content of N, at %
PLA initial	2.00 ± 0.10	
PLA + plasma O_2	2.43 ± 0.12	
PLA + plasma N_2	2.08 ± 0.10	1.60 ± 0.08
PLA + plasma Ar	2.31 ± 0.11	

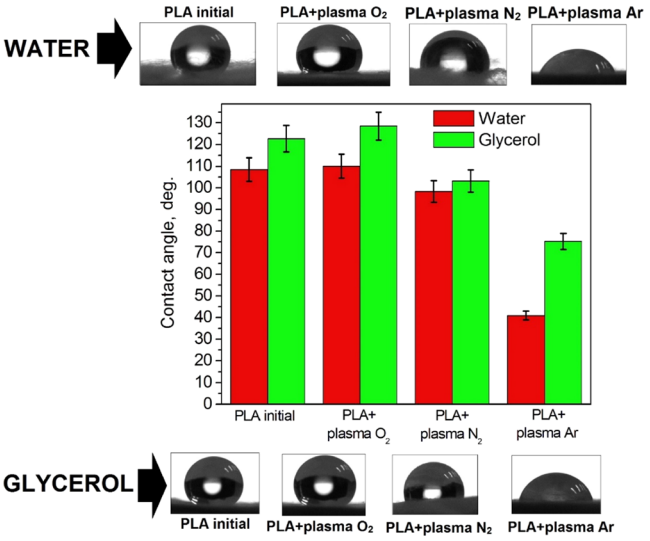

Figure 7. Water and glycerol contact angle of PLA-based scaffolds.

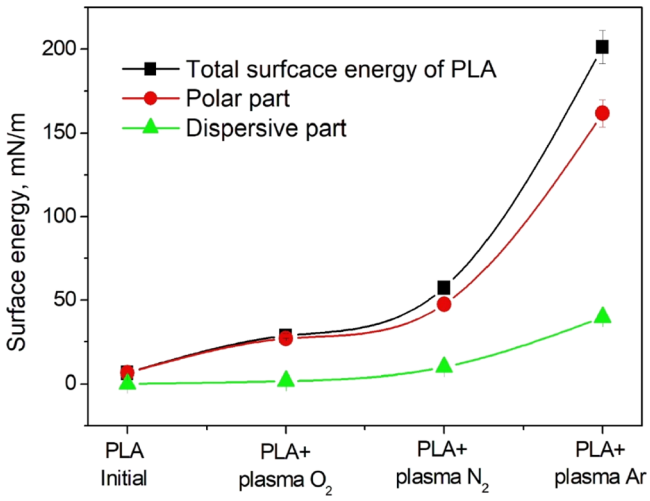

Figure 8. Surface energy of PLA before and after plasma treatment.

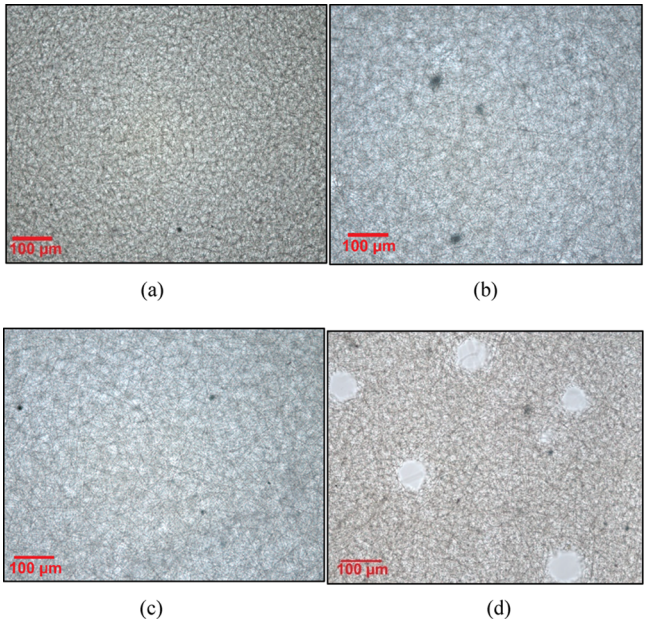

Figure 9. Microphotographs of PLA-based scaffolds before and after plasma treatment: (a) initial and after plasma treatment in (b) oxygen, (c) nitrogen, and (d) argon.

with oxidation processes in the surface layer after plasma exposure. The enhancement in surface energy can be taken as evidence for improvement in adhesion of the material.

3.3. Microstructure of the PLA Surface. Microphotographs of the PLA-based scaffolds before and after plasma treatment are shown in Figure 9. Both initial and plasma-treated PLA show a fibrous structure, but oxygen- and nitrogen plasma-treated scaffolds show defects located unevenly on the surface. Argon plasma modification leads to the formation of volume defects ~30 μm in size uniformly over the surface (Figure 9d). This defect structure may have a positive effect on cell adhesion and viability.[15]

Following analysis of the physicochemical characteristics of PLA-based scaffolds, we conducted some biological studies of the argon plasma-modified samples, the chemical composition and morphology of which were significantly changed by plasma treatment. Thus, the cell viability and pro-/anti-inflammatory activity were assessed for unmodified and argon plasma-modified PLA scaffolds.

3.4. Effect of Scaffolds on Macrophage Activation and Viability. Macrophages are key cells of the innate immune system. They play a major role in the body's response to the implanted material. Macrophages phagocytose wear particles on the surface of articular prostheses, initiate inflammation in the prosthetic zone and osteolysis, and control the formation of a fibrous capsule around foreign bodies. Some resident tissue macrophages originate from monocytes that circulate in the blood and receive their first differentiation and activation signal during circulation.[16] Activation of tissue macrophages and their subsequent immunological functions are determined by the local immune status in the cell microenvironment and occur in two main directions: along the classical activation pathway (M1 activation) and along an alternative activation pathway (M2 activation).[17] M1 activation induces a cascade of immunological reactions leading to the development of inflammation and tissue damage and is accompanied by increased secretion of proinflammatory cytokines. Recent studies have shown that M1 macrophages also exhibit reparative properties: they stimulate angiogenesis and the formation of granulation tissue.[18] M2 activation, in contrast, is caused by macrophages of the second type, the biological role of which is to regulate the intensity of the immune response, including through the secretion of anti-inflammatory cytokines, and leads to an increase in angiogenesis followed by tissue repair.[19] Cells of the M2 phenotype

https://doi.org/10.1021/acsami.2c11027
ACS Appl. Mater. Interfaces XXXX, XXX, XXX−XXX

are considered typical reparative macrophages; they suppress the inflammatory response and provide connective tissue remodeling. Based on the reaction of macrophages to implant materials, it is possible to draw conclusions about the rejection or acceptance of the implant by the patient's body and to predict the response of the immune system.[20]

We first investigated the biocompatibility of PLA-based scaffolds. Figure 10 shows the results of the study. In the control column

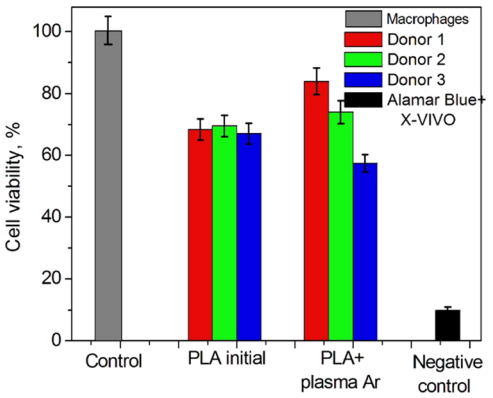

Figure 10. Effect of scaffolds on cell viability, and analysis with Alamar Blue (M0 macrophages were cocultured with the materials for 6 days in X-VIVO).

(macrophages without any materials), we combined the results for three donors into a single bin because of their equal values and took it as indicating 100% cell viability. We found that the viability of cells in the presence of the initial PLA scaffolds is less than the control but still greater than 50%. Following argon plasma modification, however, the cells of donors 1 and 2 showed viability enhanced over initial viability, and donor 3 showed the least viability in the presence of plasma-treated PLA among all samples. We conclude that plasma modification can be applied to implants made from PLA-based scaffolds as a technique for surface property improvement, but preliminary studies of individual cell viability should be carried out.

To assess the effect of scaffolds on macrophages, we investigated their influence on M1-associated cytokine release. TNFα, IL1β, and IL6 were chosen as proinflammatory (M1-associated) markers.

TNFα is an inflammatory cytokine produced by macrophages/monocytes during acute inflammation and is responsible for a diverse range of signaling events within cells, leading to necrosis or apoptosis. Our studies of the effect of scaffolds on TNF-α expression showed that during the entire period of cell cultivation, the concentration of analyzed cytokine for M0, M1, and M2 macrophage activation in the presence of both initial and Ar-modified PLA scaffolds is below the control level (Figure 11). For M2 activation of macrophages (conditions for suppressing inflammation), there is a decrease in the concentration of TNF-α in the control by a factor of 2−3 compared to M0- and M1-activated macrophages. Note that TNF-α expression in the presence of Ar-treated PLA is always lower than in the presence of untreated PLA. PLA scaffolds downregulate TNFα production by M1 and M2 macrophages on day 6.

IL-6 is the main mediator of acute inflammation secreted by macrophages. IL-6 is rapidly synthesized in response to infection or tissue damage caused by burns and trauma and activates an acute immune response. Analysis of the expression of IL-6 showed that samples of the studied scaffolds did not cause an increase in expression of the analyzed cytokine after 6 days of culturing cells on the surface of samples (Figure 12). For M0, M1, and M2 macrophage activation, the concentration of IL-6 in the presence of scaffolds is comparable to the control level, which suggests that the PLA samples (both unmodified and modified) do not affect increased production of acute inflammation mediators.

IL-1β is the predominant form of IL-1, which belongs to a group of proinflammatory cytokines. It is one of the first to be included in the body's defense response under the action of pathogenic factors. It is synthesized and secreted mainly by macrophages and monocytes. IL-1β also induces ICAM-1 expression, growth, and differentiation of B and T cells.[21] Analysis of IL-1β expression shows that for unstimulated macrophages, Ar-treated PLA scaffolds suppress the production of IL-1β compared to unmodified PLA. For M1 macrophages, the concentration of IL-1β in the presence of PLA-based scaffolds decreases to the same level as the Ar-modified samples (Figure 13). The secretion of IL-1β M2 by macrophages in the control compared with M0 decreases by a factor of ∼4. The concentration of IL-1β in the presence of samples also decreases compared with M0 and M1, indicating that PLA in both states—unmodified and modified—does not have a permanent inflammatory effect under conditions of suppression of inflammation.

IL-10 is a cytokine with anti-inflammatory properties and plays a central role in infection by limiting the immune response to pathogens and thereby preventing damage to the host. IL10 was chosen for markers of M2.[22] Our studies of the effect of scaffolds on the expression of IL-10 show that the materials do not cause increased expression of the analyzed cytokine—the concentration of IL-10 in the presence of the initial and Ar-modified PLA is below the control level (Figure 14). The anti-inflammatory effect of IL-10 affects the wound healing process by decreasing the inflammatory response, but in the case of PLA-based scaffolds we can conclude that the materials do not induce increased IL-10 production and thus have no anti-inflammatory effect.

4. DISCUSSION

We have explored the effect of oxygen, nitrogen, and argon plasma treatment on the surface physicochemical and biological properties of PLA-based scaffolds. We find that plasma treatment influences the elemental compound and structural-phase composition. XPS analysis shows that the carbonyl bond content in the C1s spectra of the PLA surface layer decreases

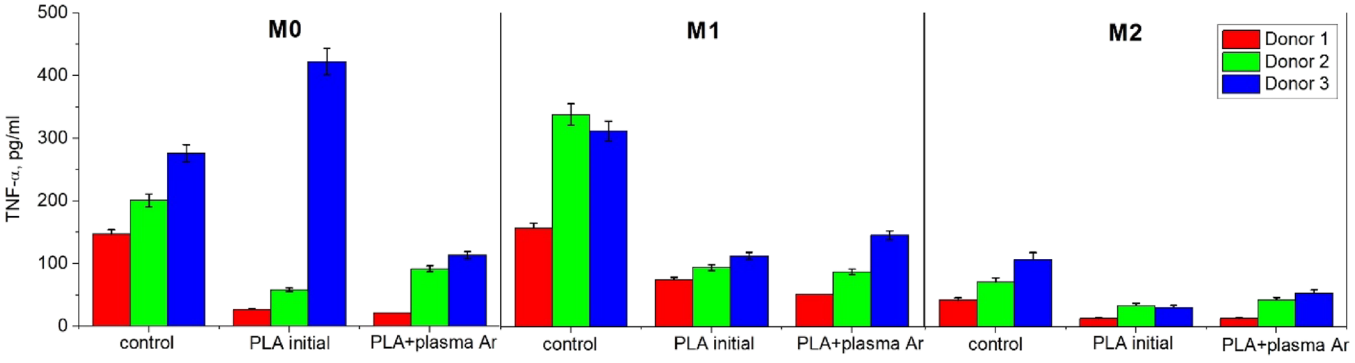

Figure 11. Effect of polylactide-based scaffolds on TNFα expression by macrophages for M0, M1, and M2 macrophage activation.

https://doi.org/10.1021/acsami.2c11027
ACS Appl. Mater. Interfaces XXXX, XXX, XXX−XXX

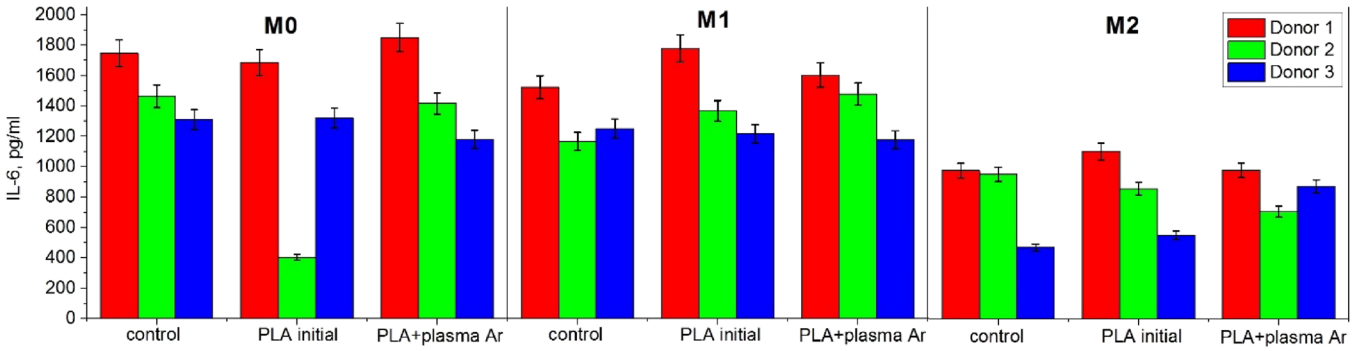

Figure 12. Effect of PLA-based scaffolds on IL-6 expression by macrophages for M0, M1, and M2 macrophage activation.

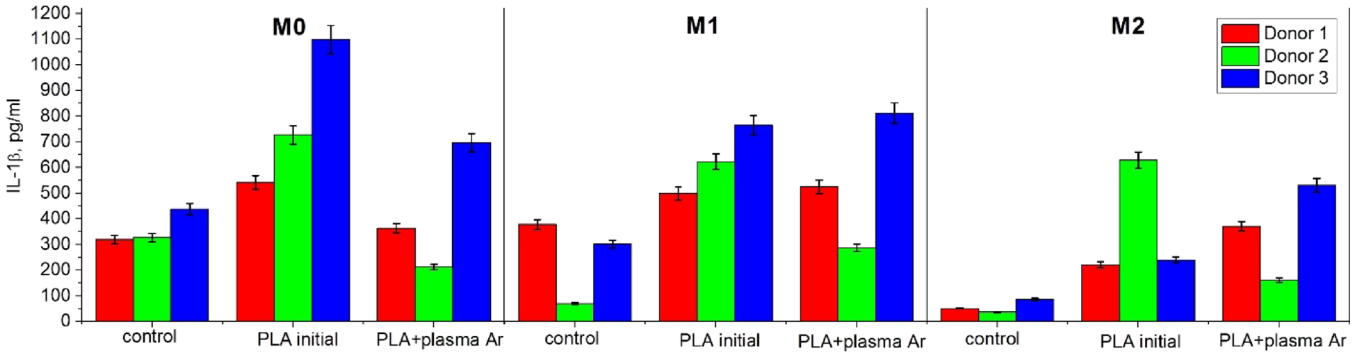

Figure 13. Effect of PLA-based scaffolds on IL-1β expression by macrophages for M0, M1, and M2 macrophage activation.

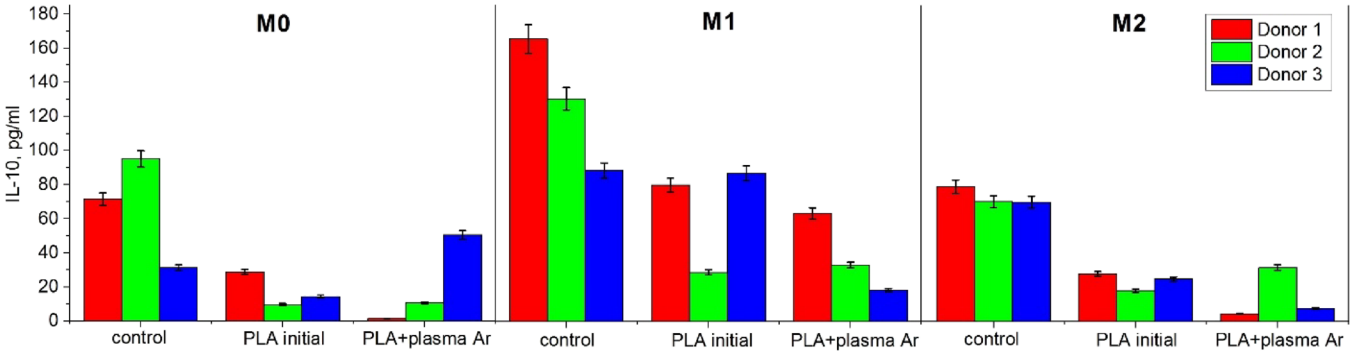

Figure 14. Effect of PLA-based scaffolds on IL-10 expression by macrophages for M0, M1, and M2 macrophage activation.

after plasma treatment, indicating the destruction of polymer bonds, for all three of the plasma-forming gases used. Along with that, carbon atomic concentration increases indicating the carbonization process of the PLA surface after plasma modification. The processes of bond rupture and crosslinking may occur simultaneously in the plasma treatment conditions. First, the interaction of the PLA surface with charged particles of plasma leads to chain scission and free radical formation. Next, free radicals with carbon terminal atoms can recombine with formation of crosslink resulting in carbonization of the modified surface layer.[23] For nitrogen plasma treatment, atomic nitrogen appears on the surface of PLA scaffolds with an atomic concentration of 1.60 at %.

Barrier discharge plasma treatment results in improvement of wettability characteristics. The contact angle is for the most part decreased (except for oxygen plasma treatment), and the total surface energy increases in all cases. The greatest changes were for argon plasma modification, for which the PLA contact angle decreases by 62% and surface energy increases by more than a factor of 30. The wettability improvement is influenced by the change in surface morphology under plasma treatment conditions. In its turn, wettability improvement plays an important role in cell adhesion and survivability.

Our results show that the viability of cells in the presence of both unmodified and plasma-modified PLA is reduced compared to the control, while remaining higher than the negative control. Investigation of the effect of unmodified and modified PLA scaffolds on the secretion of proinflammatory (TNFα, IL-6, IL-1β) cytokines by primary human macrophages using enzyme multiplied immunoassay showed that our materials did not cause increased expression of the analyzed cytokines after 6 days of cell cultivation on the PLA surface in both states—unmodified and modified. At the same time, the PLA scaffolds do not affect the increased production of anti-inflammatory cytokines (IL-10). Thus, we conclude that the material after low-temperature barrier discharge Ar-plasma modification remains immunotolerant, and the surface treat-

https://doi.org/10.1021/acsami.2c11027
ACS Appl. Mater. Interfaces XXXX, XXX, XXX−XXX

ment can be endorsed as a physicochemical property improvement technique.

5. CONCLUSIONS

Overall, our data show the effective alteration of physicochemical properties and biocompatibility of PLA-based scaffolds via low-temperature plasma treatment. The plasma-modified PLA reveals improved wettability characteristics, namely, the contact angle decrease and surface energy increase. These features affect the biocompatibility of PLA-based scaffolds. Cells are able to survive in the presence of the PLA scaffolds after argon plasma treatment, as well as this material does not cause production of both proinflammatory (TNFα, IL-6, IL-1β) and anti-inflammatory cytokines (IL-10).

AUTHOR INFORMATION

Corresponding Author

Irina A. Kurzina − *National Research Tomsk State University, Tomsk 634050, Russia;* orcid.org/0000-0003-4976-2295; Email: kurzina99@mail.ru

Authors

Olesya A. Laput − *National Research Tomsk State University, Tomsk 634050, Russia;* orcid.org/0000-0001-5553-5983

Irina V. Vasenina − *P.N. Lebedev Physical Institute, Moscow 119333, Russia;* orcid.org/0000-0001-8768-3403

Yelena G. Shapovalova − *National Research Tomsk State University, Tomsk 634050, Russia;* orcid.org/0000-0003-3640-7040

Andrey N. Ochered'ko − *Institute of Petroleum Chemistry SB RAS, Tomsk 634055, Russia;* orcid.org/0000-0001-5629-064X

Aleksandr V. Chernyavskii − *MIREA—Russian Technological University, Moscow 119454, Russia;* orcid.org/0000-0002-4020-613X

Sergey V. Kudryashov − *Institute of Petroleum Chemistry SB RAS, Tomsk 634055, Russia;* orcid.org/0000-0002-6734-2123

Complete contact information is available at: https://pubs.acs.org/10.1021/acsami.2c11027

Notes

The authors declare no competing financial interest.

ACKNOWLEDGMENTS

This work was supported the Tomsk State University Development Program (Priority-2030) and partially funded by the Ministry of Science and Higher Education of the Russian Federation. The study was funded by RFBR, project number 20-32-90175 (Section 3.4). Special thanks to the Scientific and Educational Center named after B.P. Weinberg of the National Research Tomsk Polytechnic University, and particularly to Associate Professor S.I. Tverdokhlebov and Research Officer E. N. Bolbasov, and personally to I. G. Brown for assistance and support.

REFERENCES

(1) Hu, X.; Liu, S.; Zhou, G.; Huang, Y.; Xie, Z.; Jing, X. Electrospinning of Polymeric Nanofibers for Drug Delivery Applications. *J. Controlled Release* **2014**, *185*, 12−21.

(2) Garric, X.; Guillaume, O.; Dabboue, H.; Vert, M.; Moles, J. P. Potential of a PLA−PEO−PLA-Based Scaffold for Skin Tissue Engineering: InVitro Evaluation. *J Biomat Sci.* **2012**, *23*, 1687−1700.

(3) Tyler, B.; Gullotti, D.; Mangraviti, A.; Utsuki, T.; Brem, H. Polylactic Acid (PLA) Controlled Delivery Carriers for Biomedical Applications. *Adv. Drug Delivery Rev.* **2016**, *107*, 163−175.

(4) Farah, S.; Anderson, D. G.; Langer, R. Physical and Mechanical Properties of PLA, and Their Functions in Widespread Applications − A Comprehensive Review. *Adv. Drug Delivery Rev.* **2016**, *107*, 367−392.

(5) Gugutkov, D.; Gustavsson, J.; Cantini, M.; Salmeron-Sánchez, M.; Altankov, G. Electrospun Fibrinogen-PLA Nanofibres for Vascular Tissue Engineering. *J. Tissue Eng. Regener. Med.* **2017**, *11*, 2774−2784.

(6) Laput, O. A.; Vasenina, I. V.; Salvadori, M. C.; Savkin, K. P.; Zuza, D. A.; Kurzina, I. A. Low Temperature Plasma Treatment of Polylactic Acid and PLA/HA Composite Material. *J. Mater. Sci.* **2019**, *54*, 11726−11738.

(7) Souza, M. A.; Oliveira, J. E.; Medeiros, E. S.; Glenn, G. M.; Mattoso, L. H. C. Controlled Release of Linalool Using Nanofibrous Membranes of Poly(Lactic Acid) Obtained by Electrospinning and Solution Blow Spinning: A Comparative Study. *J. Nanosci. Nanotechnol.* **2015**, *15*, 5628−5636.

(8) Lao, L.; Tan, H.; Wang, Y.; Gao, C. Chitosan Modified Poly(L-Lactide) Microspheres as Cell Microcarriers for Cartilage Tissue Engineering. *Colloids Surf Biointerfaces.* **2008**, *66*, 218−225.

(9) Tverdokhlebov, S. I.; Bolbasov, E. N.; Shesterikov, E. V.; Antonova, L. V.; Golovkin, A. S.; Matveeva, V. G.; Petlin, D. G.; Anissimov, Y. G. Modification of Polylactic Acid Surface Using RF Plasma Discharge with Sputter Deposition of a Hydroxyapatite Target for Increased Biocompatibility. *Appl. Surf. Sci.* **2015**, *329*, 32−39.

(10) Botvin, V. V.; Shapovalova Ye, G.; Zenkova, E. V.; Pozdnyakov, M. A. Synthesis of Glycolic and Lactic Acid Oligomers. X International Conference of Students and Young Scientists. In *Prospects of Fundamental Sciences Development*; 2013; pp 266−268.

(11) Bico, J.; Thiele, U.; Quere, D. Wetting of Textured Surfaces. *Colloids Surf., A* **2002**, *206*, 41−46.

(12) Anderson, J. M.; Rodriguez, A.; Chang, D. T. Foreign Body Reaction to Biomaterials. *Semin. Immunol.* **2008**, *20*, 86−100.

(13) Gratchev, A.; Kzhyshkowska, J.; Köthe, K.; Muller-Molinet, I.; Kannookadan, S.; Utikal, J.; Goerdt, S. M1 and M2 Can Be Re-Polarized by Th2 or Th1 Cytokines Respectively and Respond to Exogenous Danger Signals. *Immunobiology* **2006**, *211*, 473−486.

(14) AO Vector-Best. https://vector-best.ru/en/prod/index.php?SECTION_ID=2748, 2022 (accessed January 12, 2022).

(15) Liu, R.; Zhang, S.; Zhao, C.; Yang, D.; Cui, T.; Liu, Y.; Min, Y. Regulated Surface Morphology of Polyaniline/Polylactic Acid Composite Nanofibers via Various Inorganic Acids Doping for Enhancing Biocompatibility in Tissue Engineering. *Nanoscale Res. Lett.* **2021**, *16*, 4.

(16) Gordon, S.; Taylor, P. R. Monocyte and Macrophage Heterogeneity. *Nat. Rev. Immunol.* **2005**, *5*, 953−964.

(17) Murray, P. J.; Allen, J. E.; Biswas, S. K.; Fisher, E. A.; Gilroy, D. W.; Goerdt, S.; Gordon, S.; Hamilton, J. A.; Ivashkiv, L. B.; Lawrence, T.; Locati, M.; Mantovani, A.; Martinez, F. O.; Mege, J. L.; Mosser, D. M.; Natoli, G.; Saeij, J. P.; Schultze, J. L.; Shirey, K. A.; Sica, A.; Suttles, J.; Udalova, I.; van Ginderachter, J. A.; Vogel, S. N.; Wynn, T. A. Macrophage Activation and Polarization: Nomenclature and Experimental Guidelines. *Immunity* **2014**, *41*, 14−20.

(18) Spiller, K. L.; Anfang, R. R.; Spiller, K. J.; Ng, J.; Nakazawa, K. R.; Daulton, J. W.; Vunjak-Novakovic, G. The Role of Macrophage Phenotype in Vascularization of Tissue Engineering Scaffolds. *Biomaterials* **2014**, *35*, 4477−4488.

(19) Kzhyshkowska, J.; Gudima, A.; Riabov, V.; Dollinger, C.; Lavalle, P.; Vrana, N. E. Macrophage Responses to Implants: Prospects for Personalized Medicine. *J. Leukocyte Biol.* **2015**, *98*, 953−962.

(20) Stankevich, K. S.; Gudima, A.; Filimonov, V. D.; Klüter, H.; Mamontova, E. M.; Tverdokhlebov, S. I.; Kzhyshkowska, J. Surface Modification of Biomaterials Based on High-Molecular Polylactic Acid and Their Effect on Inflammatory Reactions of Primary Human

Monocyte-Derived Macrophages: Perspective for Personalized Therapy. *Mater. Sci. Eng., C* **2015**, *51*, 117−126.
(21) Akira, S.; Hirano, T.; Taga, T.; Kishimoto, T. Biology of Multifunctional Cytokines: IL 6 and Related Molecules (IL 1 and TNF). *FASEB J.* **1990**, *4*, 2860−2867.
(22) Saraiva, M.; O'Garra, A. The Regulation of IL-10 Production by Immune Cells. *Nat. Rev. Immunol.* **2010**, *10*, 170−181.
(23) Laput, O. A.; Vasenina, I. V.; Botvin, V. V.; Kurzina, I. A. Surface Modification of Polylactic Acid by Ion, Electron Beams and Low-Temperature Plasma: a Review. *J. Mater. Sci.* **2022**, *57*, 1−2361.

https://doi.org/10.1021/acsami.2c11027
ACS Appl. Mater. Interfaces XXXX, XXX, XXX−XXX